SUPPLEMENTARY INFORMATION

Preparation and Structure of NHC Hg(II) and Ag(I) Macrometallocycles

Qing-Xiang Liu,* Rui Liu, Yue Ding, Xiao-Jun Zhao, Zhi-Xiang Zhao, Wei Zhang

Tianjin Key Laboratory of Structure and Performance for Functional Molecules; Key Laboratory of Inorganic-Organic Hybrid Functional Material Chemistry, Ministry of Education; College of Chemistry, Tianjin Normal University, Tianjin 300387, China.

* Corresponding author, E-mail: tjnulqx@163.com

Contents

1. CCDC numbers for complexes 1-7

CCDC 1012248-1012254 contains the supplementary crystallographic data for complexes complexes **1-7**. These data can be obtained free of charge via http://www.ccdc.cam.ac.uk/conts/retrieving.html, or from the Cambridge Crystallographic Data Centre, 12 Union Road, Cambridge, CB2 1EZ, UK; fax: (+44) 1223-336-033; or e-mail: deposit@ccdc.cam.ac.uk.

2. The slip angles and the bond distances of O(2)-metal for complexes 1-7

Table S1 The slip angles between O(2) and anthraquinone plane, and the bond distances of O(2)-Metal for **1-7**

Complexes	slip angles (˚)	O(2)-metal (Å)
1	9.9(8)	2.942(8)
2	16.5(1)	2.845(6)
3	15.6(7)	2.827(6)
4	12.9(9)	2.879(8)
5	16.5(9)	2.954(1)
6	13.7(3)	3.042(6)
7	11.8(6)	2.632(4)

3. The dihedral angles of complexes 1-7

Table S2 In the same ligand of **1-7**, the dihedral angles (˚) between anthraquinone plane and two imidazole (or benzimidazole) rings (A), the dihedral angles (˚) between benzene (or pyridine) rings and the adjacent imidazole (or benzimidazole) rings (B), and the dihedral angles between two imidazole (or benzimidazole) rings (C)

Complexes	A	B	C
1	70.3(8), 70.9(3), 73.7(7), 77.8(7)	79.5(5), 79.9(8), 82.4(0), 88.9(0)	20.7(1))
2	53.2(2), 70.0(8)	75.1(7), 77.6(3)	17.6(2)
3	77.4(7), 84.1(6)	_	21.1(7)

4	60.4(5), 64.3(8)	60.7(7), 73.4(3)	7.1(3)
5	74.4(6), 85.6(5)	_	12.0(4)
6	59.9(1), 85.4(3)	_	39.8(7)
7	60.1(1), 64.6(5)	82.9(7), 83.7(6)	7.7(1)

4. H-Bonding geometry for complexes 1, 2 and 4-7.

Table S3 H-Bonding Geometry (Å, °) for complexes **1**, **2** and **4-7**

	D-H···A	D-H	H···A	D···A	D-H···A
1	C(12)-H(12B)···Br(1)^{i}	0.990(0)	2.862(4)	3.763(9)	151.7(6)
	C(22)-H(22)···Br (8)^{i}	0.950(0)	2.832(8)	3.590(6)	137.5(7)
2	C(18)-H(18)···O (3)^{ii}	0.950(1)	2.286(1)	3.150(6)	150.9(3)
4	C(11)-H(11)···I(6)^{i}	0.949(8)	2.894(3)	3.757(1)	151.5(9)
	C(39)-H(39A)···O(3)^{ii}	0.988(8)	2.574(6)	2.951(0)	102.5(0)
	C(14)-H(14B)···I(4)^{i}	0.989(1)	3.027(0)	3.879(9)	145.1(1)
5	C(22)-H(22A)···F(6)^{i}	0.990(8)	2.499(8)	3.075(3)	116.7(1)
	C(4)-H(4)···F(1)^{i}	0.951(2)	2.498(9)	3.319(6)	144.5(1)
	C(28)-H(28B)···F(5)^{i}	0.980(4)	2.489(1)	3.335(3)	144.3(8)
6	C(8)-H(8)···F (1)^{i}	0.949(6)	2.500(5)	3.385(4)	155.0(8)
7	C(12)-H(12)···O(3)^{i}	0.949(5)	2.593(5)	3.269(1)	128.0(4)
	C(39)-H(39A)···N(1)^{i}	0.990(2)	2.590(0)	3.520(3)	156.5(0)
	C(37)-H(37)···F(1)^{i}	0.950(1)	2,422(1)	3.311(2)	155.7(0)
	C(6)-H(6)···F(4)^{i}	0.990(9)	2.536(3)	3.327(8)	136.7(2)

Symmetry code: i: *x*, -2 + *y*, *z* for **1**; ii: -2 + *x*, *y*, -1 + *z* for **2**; i: -1 + *x*, *y*, -1 + *z*; ii: -0.5 + *x*, 1.5 - *y*, -0.5 + *z* for **4**; i: 2 - *x*, 2 - *y*, -2 - *z* for **5**; i: -1 + *y*, -*x* + *y*, -*z* for **6**; i: 3 + *x*, *y*, -1 + *z* for **7**.

5. The distances of π-π interactions, and the distances and angles of C-H···π contacts for complexes 2, 3 and 6.

Table S4 Distances (Å) of π-π interactions, and distances (Å) and angles (˚) of C-H···π contacts for complexes **2**, **3** and **6**

Complexes	π-π		C-H···π	
	face-to-face	center-to-center	H···π	C-H···π
2	_	_	2.440(8)	166.7(8)
3	3.547(1) (imidazole) 3.513(5) (anthraquinone)	3.959(6) (imidazole) 3.613(5) (anthraquinone)	_	_
6	3.393(1) (benzimidazole, anthraquinone)	3.772(6) (benzimidazole, anthraquinone)	_	_

6. Electrochemical data for precursors $L^1H_2\cdot(PF_6)_2$, $L^3H_2\cdot(PF_6)_2$ and $L^4H_2\cdot(PF_6)_2$, and complexes 5-7

Table S5. Electrochemical data in room temperature for precursors $L^1H_2\cdot(PF_6)_2$, $L^3H_2\cdot(PF_6)_2$ and $L^4H_2\cdot(PF_6)_2$, and complexes **5-7** in CH_3CN using 0.1 M $^nBu_4NBF_4$

Compounds	Solvent	E^{o1} (V) vs. SCE	E^{o2} (V) vs. SCE
$L^1H_2\cdot(PF_6)_2$	CH_3CN	-0.94	-1.45
5	CH_3CN	-0.63	-1.06
$L^3H_2\cdot(PF_6)_2$	CH_3CN	-0.99	-1.72
6	CH_3CN	-0.98	-1.66
$L^4H_2\cdot(PF_6)_2$	CH_3CN	-0.99	-1.73
7	CH_3CN	-0.99	-1.68

7. Cyclic voltammograms of precursors $L^1H_2\cdot(PF_6)_2$, $L^3H_2\cdot(PF_6)_2$ and $L^4H_2\cdot(PF_6)_2$.

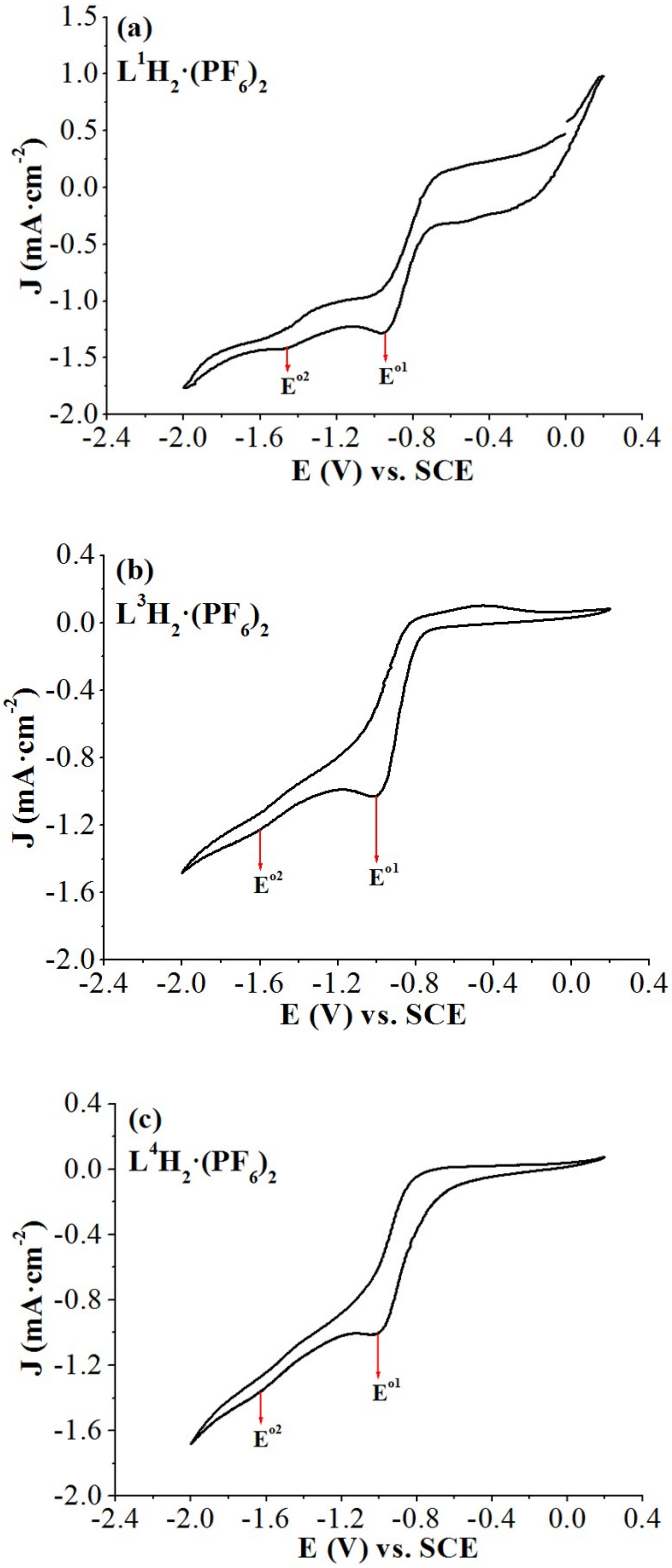

Fig. S1 Cyclic voltammograms of precursors $\mathbf{L^1H_2\cdot(PF_6)_2}$, $\mathbf{L^3H_2\cdot(PF_6)_2}$ and $\mathbf{L^4H_2\cdot(PF_6)_2}$ in CH_3CN using 0.1 M $^nBu_4NBF_4$ as the supporting electrolyte.

8. The ^{1}H NMR spectra and ^{13}C NMR spectra for all intermediates, precursors

and complexes 1-7.

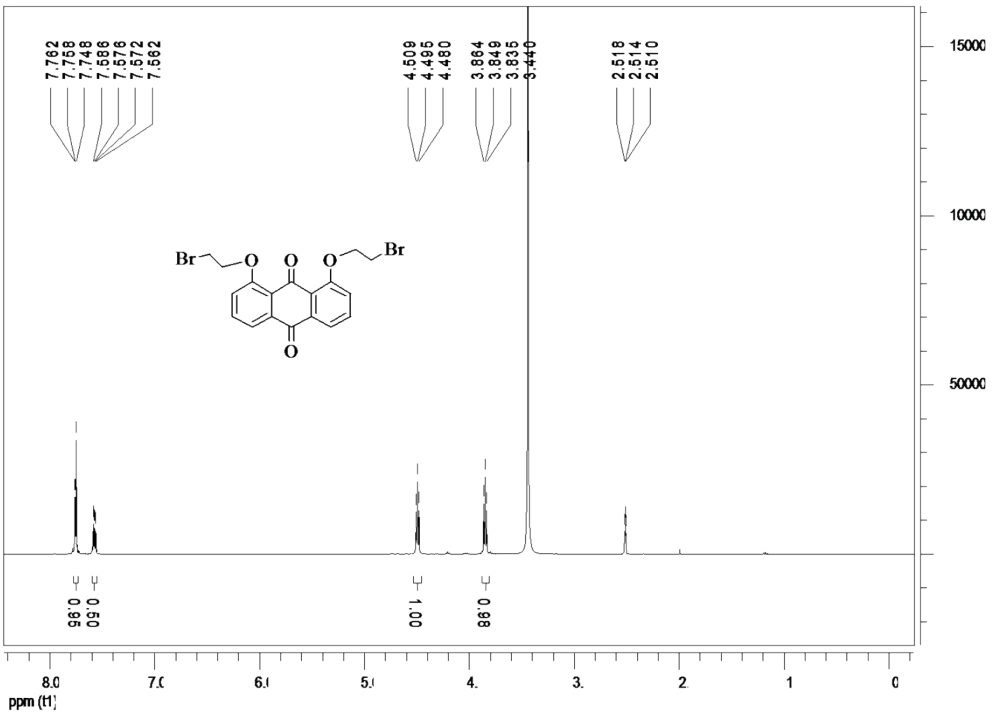

Fig. S2. The ^{1}H NMR (400 MHz, DMSO-d_6) spectrum for 1,8-bis(2-bromoethoxy)-9,10-anthraquinone.

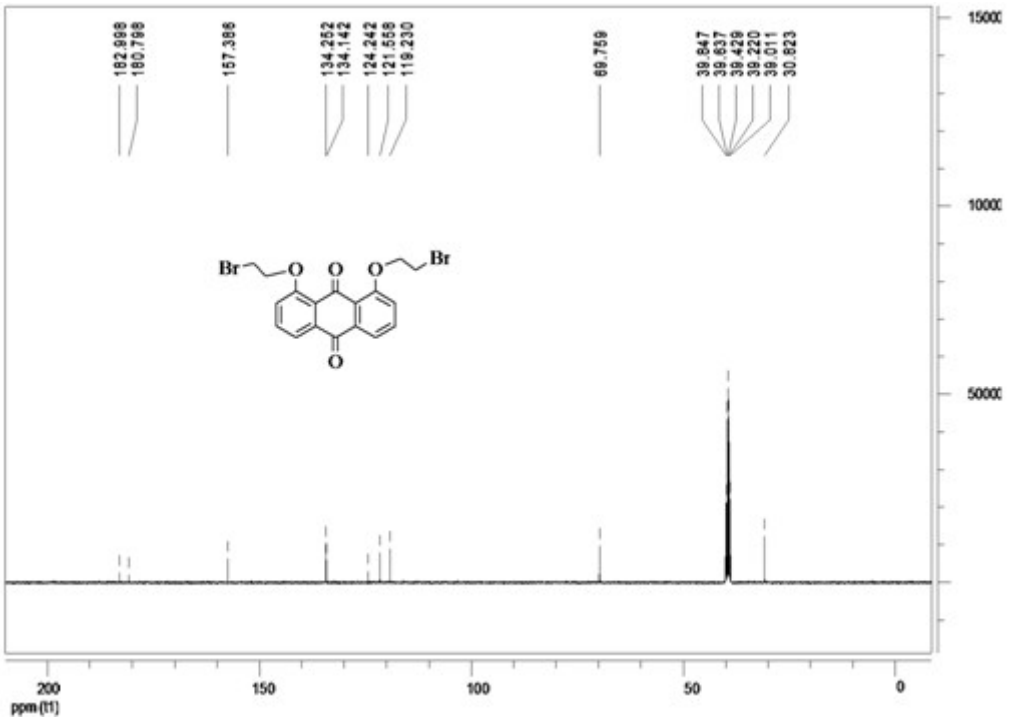

Fig. S3. The ^{13}C NMR (100 MHz, DMSO-d_6) spectrum for 1,8-bis(2-bromoethoxy)-9,10-anthraquinone.

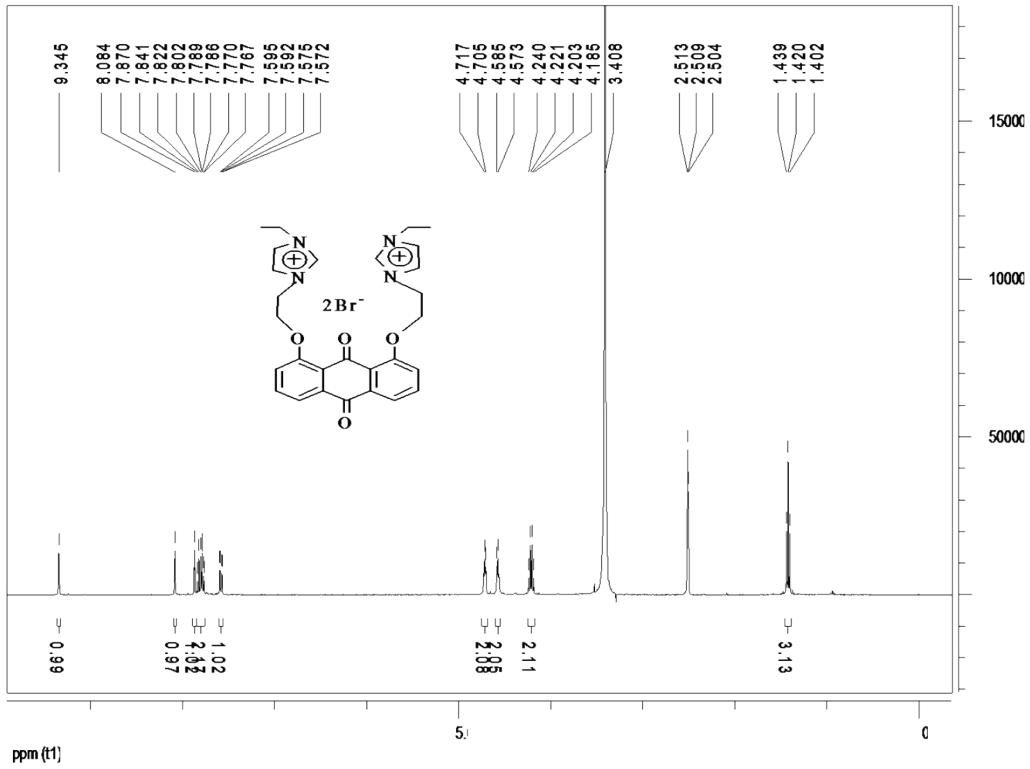

Fig. S4. The ^{1}H NMR (400 MHz, DMSO-d_6) spectrum for $\mathbf{L^1H_2{\cdot}Br_2}$.

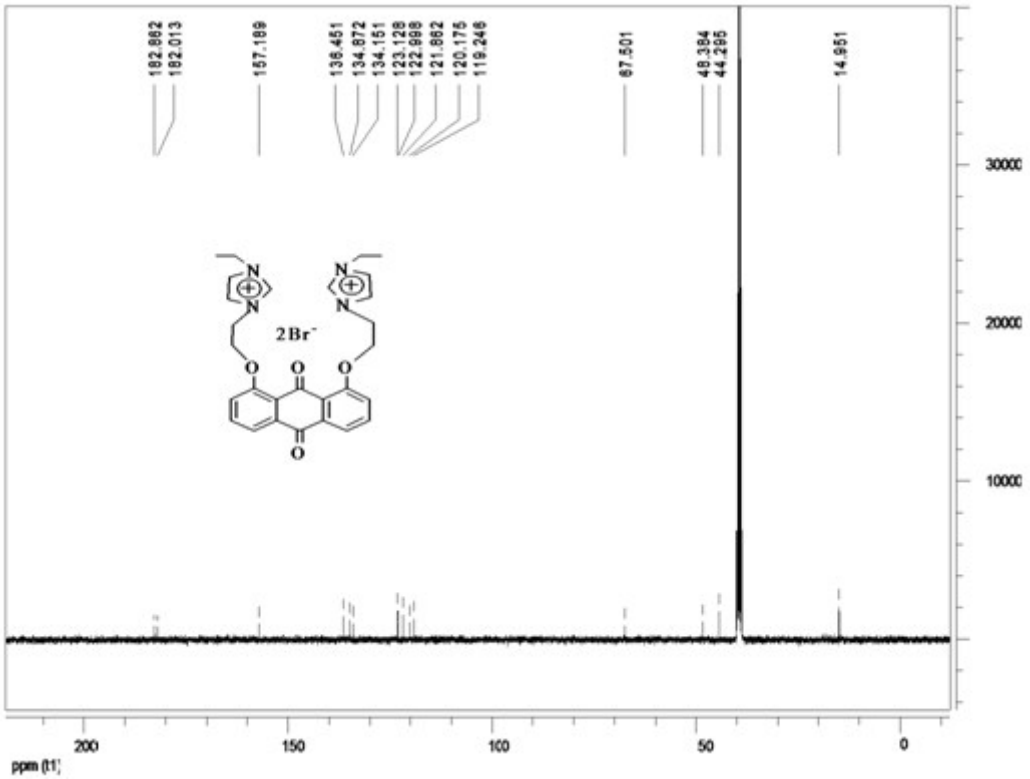

Fig. S5. The ^{13}C NMR (100 MHz, DMSO-d_6) spectrum for $\mathbf{L^1H_2{\cdot}Br_2}$.

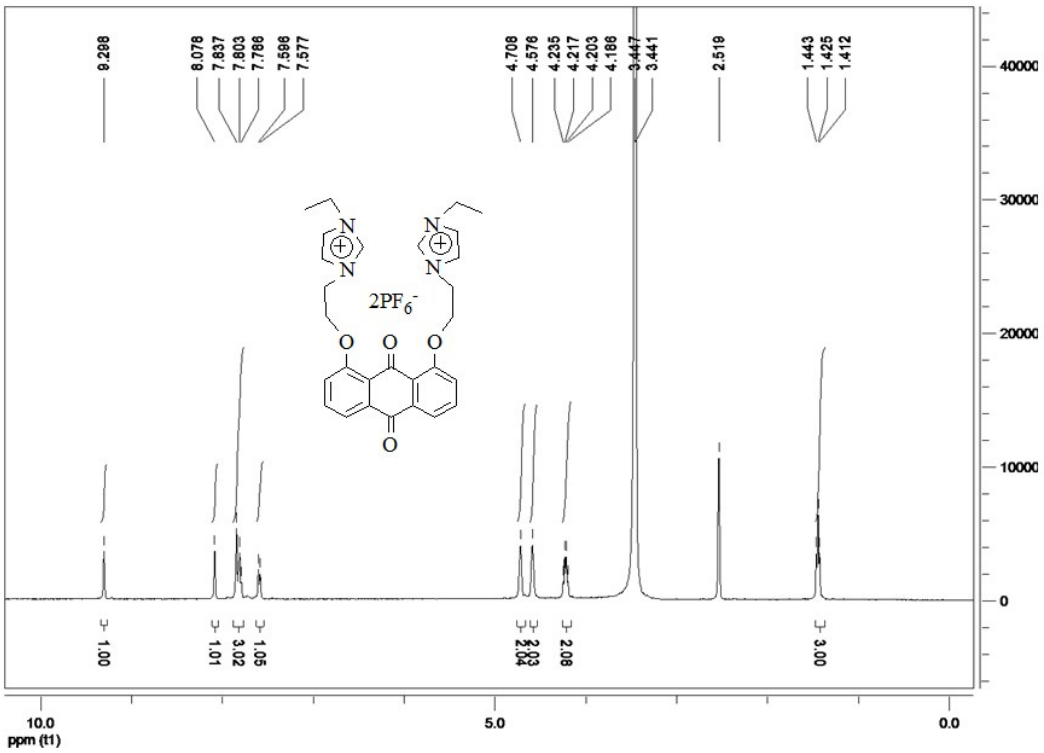

Fig. S6. The ^{1}H NMR (400 MHz, DMSO-d_6) spectrum for $\mathbf{L^1H_2{\cdot}(PF_6)_2}$.

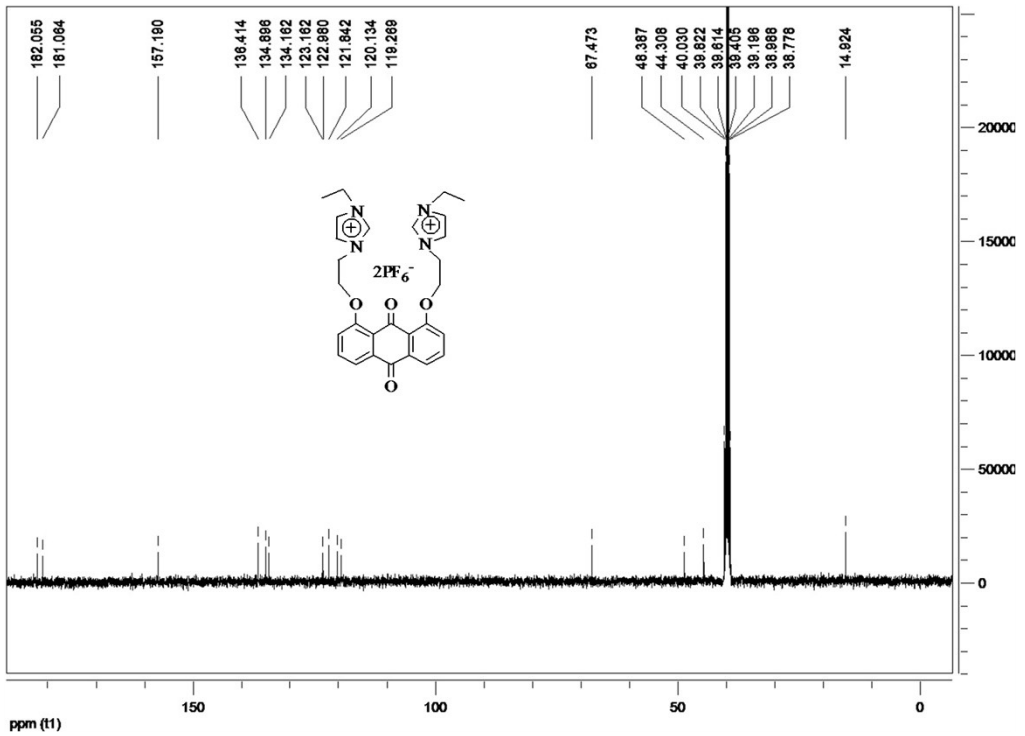

Fig. S7. The ^{13}C NMR (100 MHz, DMSO-d_6) spectrum for $\mathbf{L^1H_2{\cdot}(PF_6)_2}$.

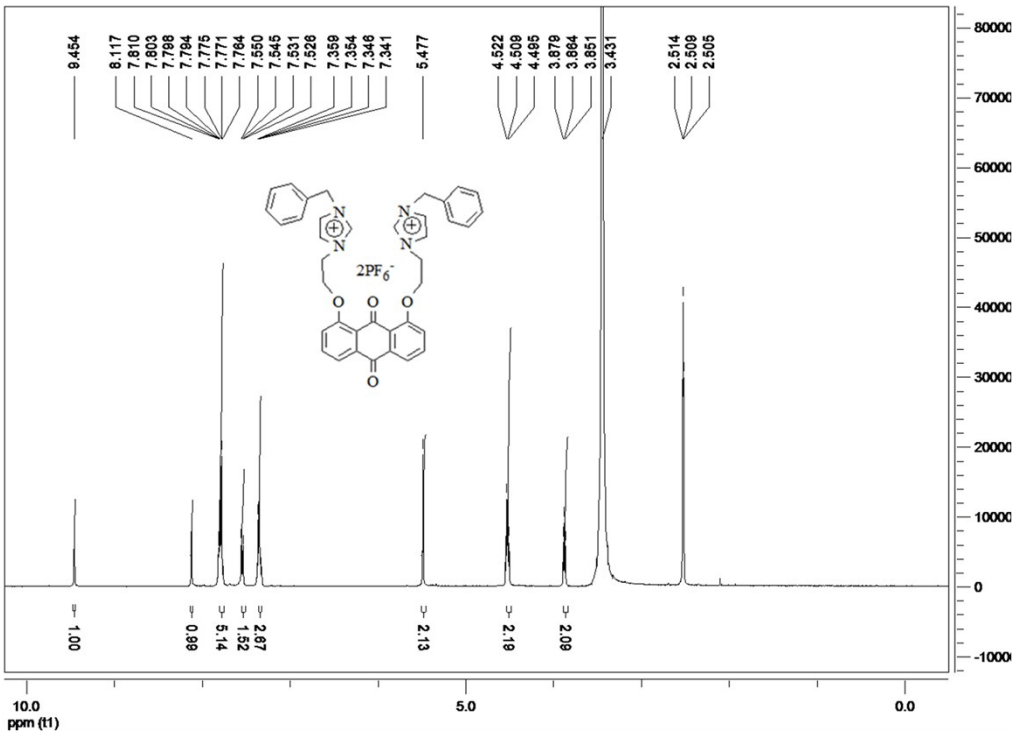

Fig. S8. The ^{1}H NMR (400 MHz, DMSO-d_6) spectrum for $\mathbf{L^2H_2{\cdot}(PF_6)_2}$.

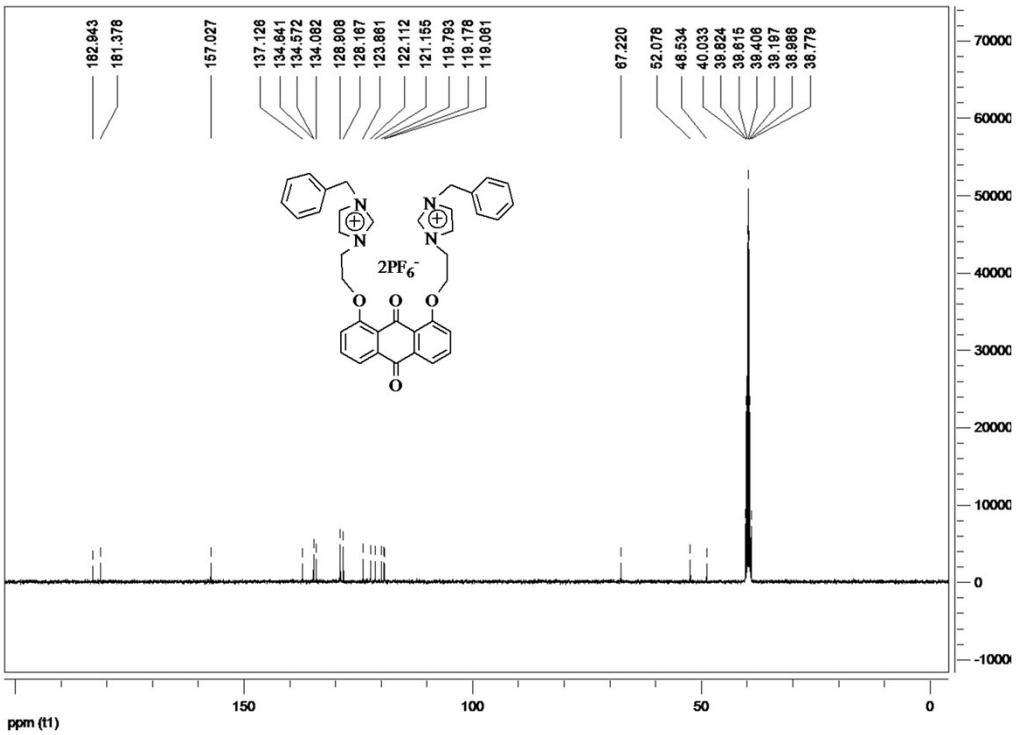

Fig. S9. The ^{13}C NMR (100 MHz, DMSO-d_6) spectrum for $\mathbf{L^2H_2{\cdot}(PF_6)_2}$.

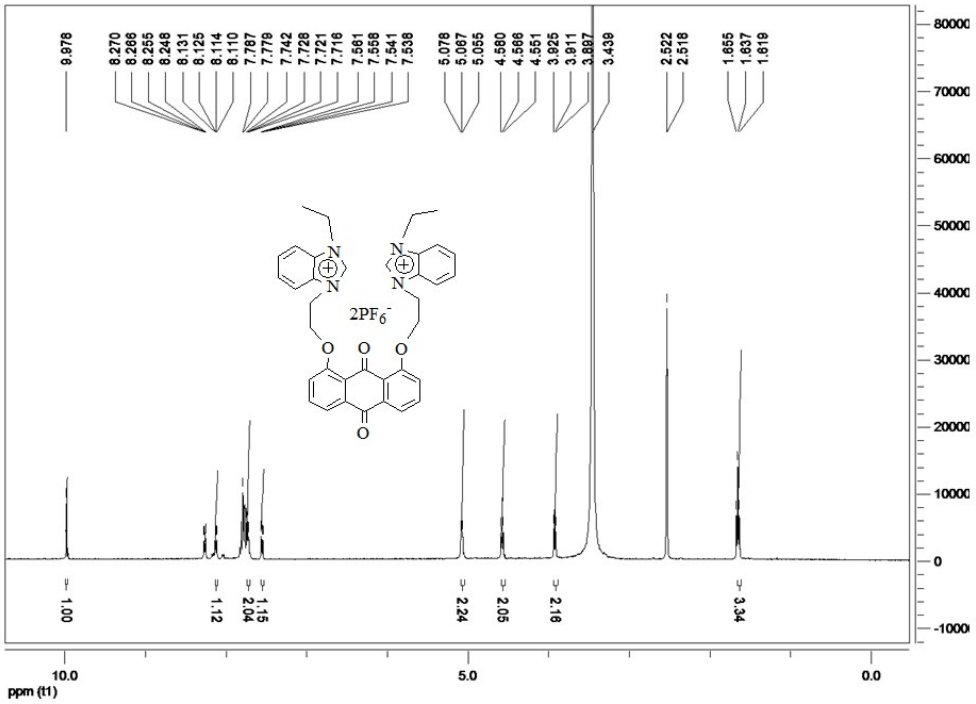

Fig. S10. The ^{1}H NMR (400 MHz, DMSO-d_6) spectrum for $\mathbf{L^3H_2 \cdot (PF_6)_2}$.

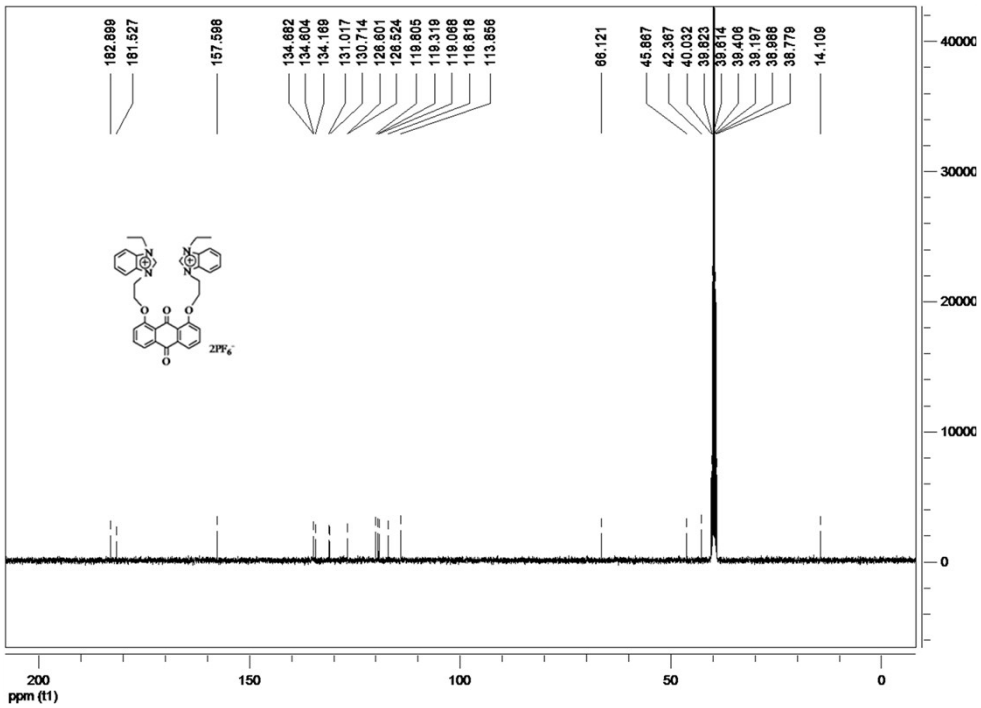

Fig. S11. The ^{13}C NMR (100 MHz, DMSO-d_6) spectrum for $\mathbf{L^3H_2 \cdot (PF_6)_2}$.

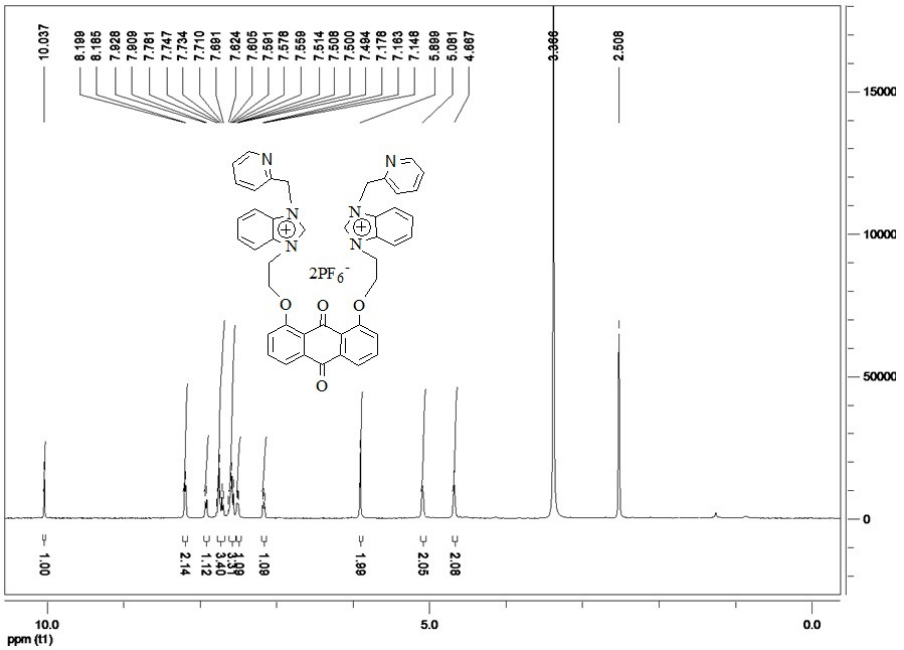

Fig. S12. The ^{1}H NMR (400 MHz, DMSO-d_6) spectrum for $\mathbf{L^4H_2 \cdot (PF_6)_2}$.

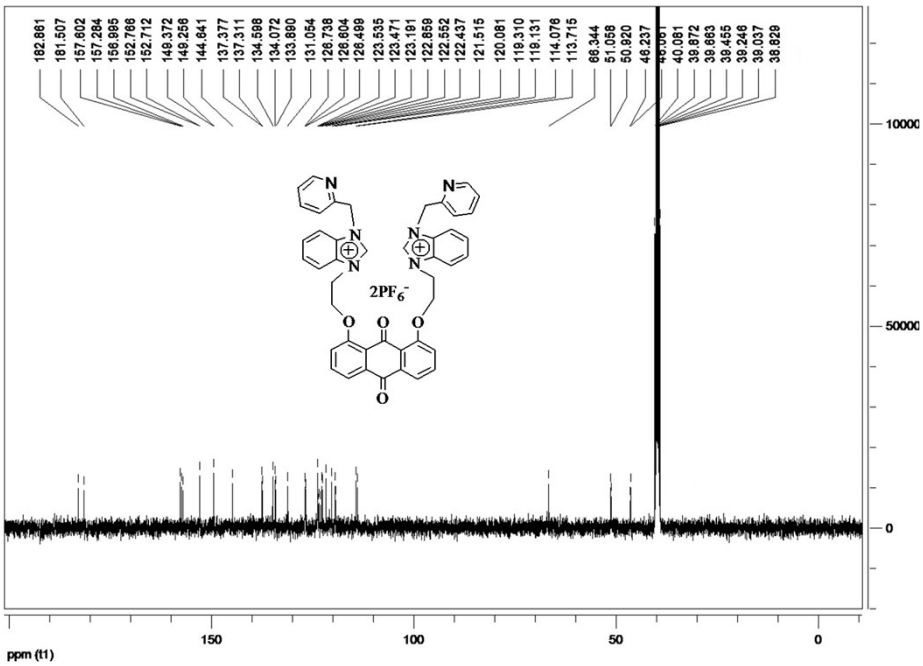

Fig. S13. The ^{13}C NMR (100 MHz, DMSO-d_6) spectrum for $\mathbf{L^4H_2 \cdot (PF_6)_2}$.

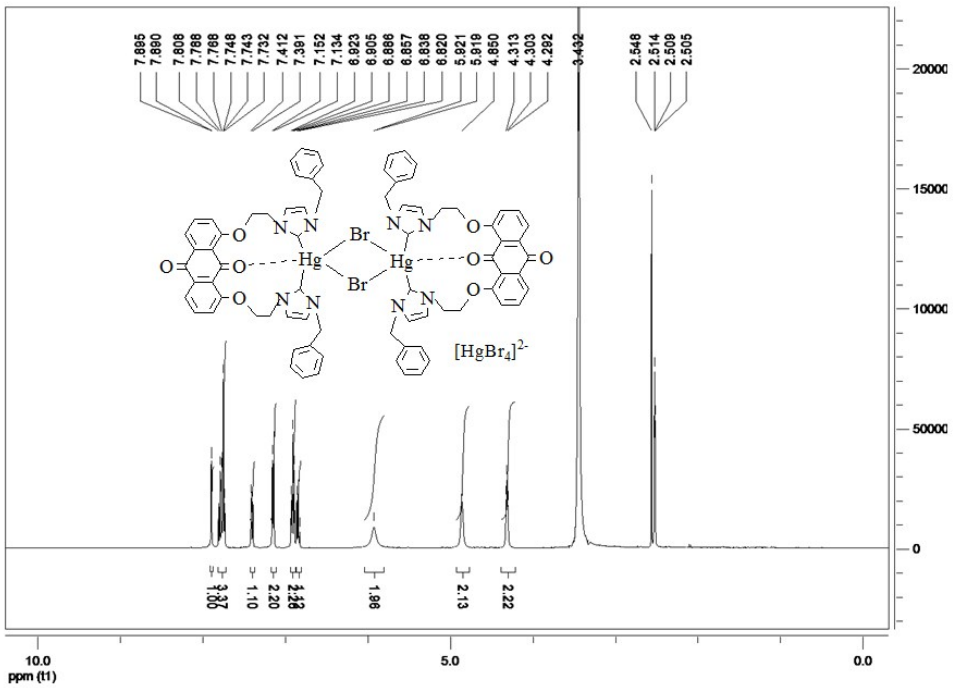

Fig. S14. The ^{1}H NMR (400 MHz, DMSO-d_6) spectrum for **1**.

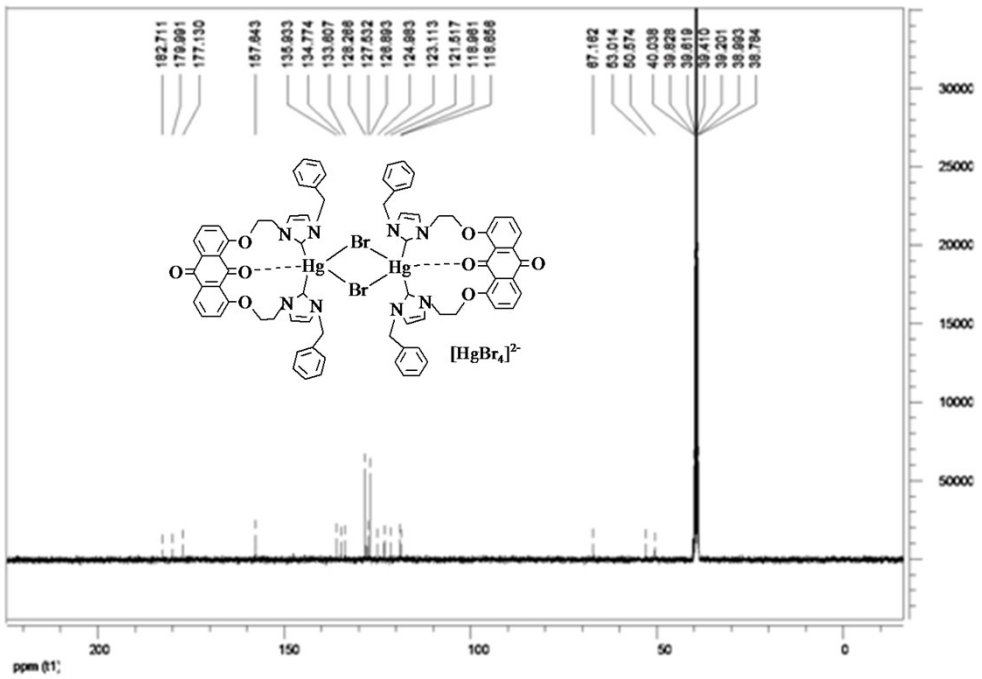

Fig. S15. The ^{13}C NMR (100 MHz, DMSO-d_6) spectrum for **1**.

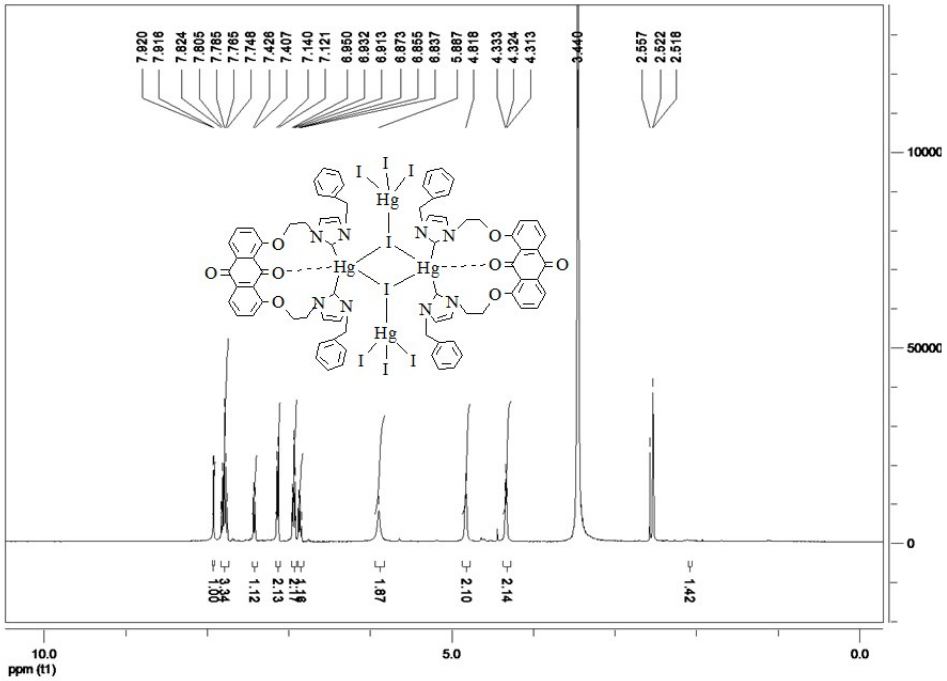

Fig. S16. The ^{1}H NMR (400 MHz, DMSO-d_6) spectrum for **2**.

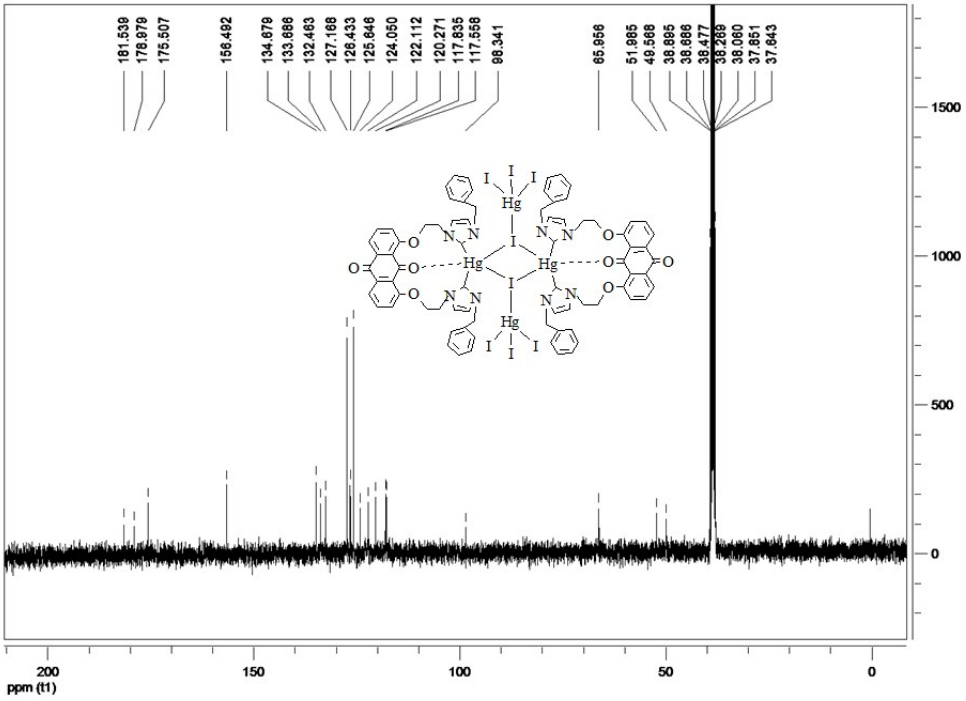

Fig. S17. The ^{13}C NMR (100 MHz, DMSO-d_6) spectrum for **2**.

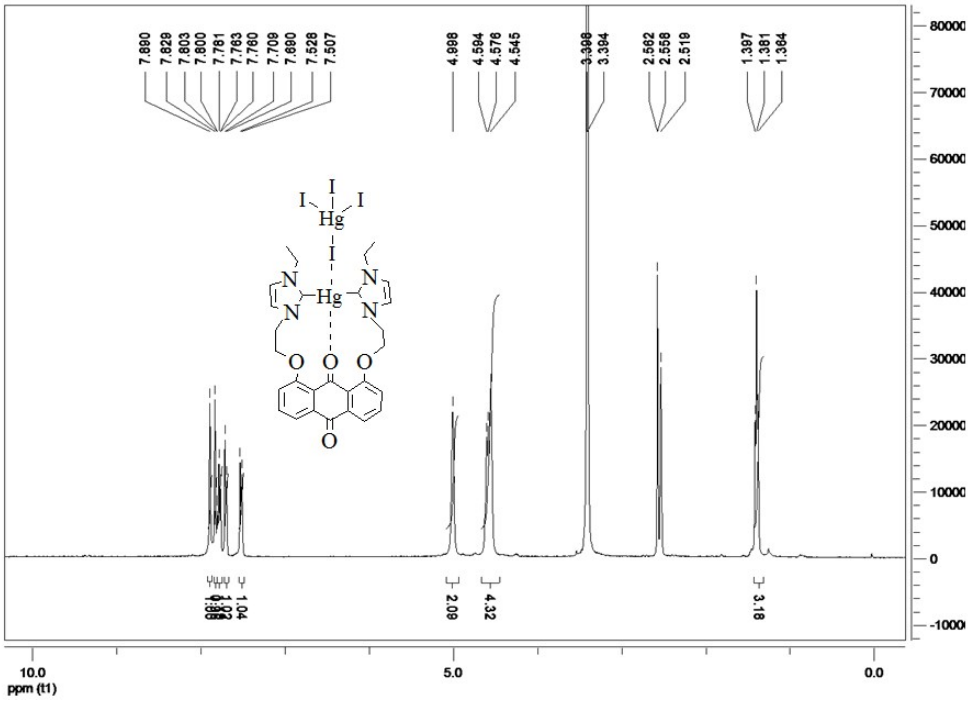

Fig. S18. The ^{1}H NMR (400 MHz, DMSO-d_6) spectrum for **3**.

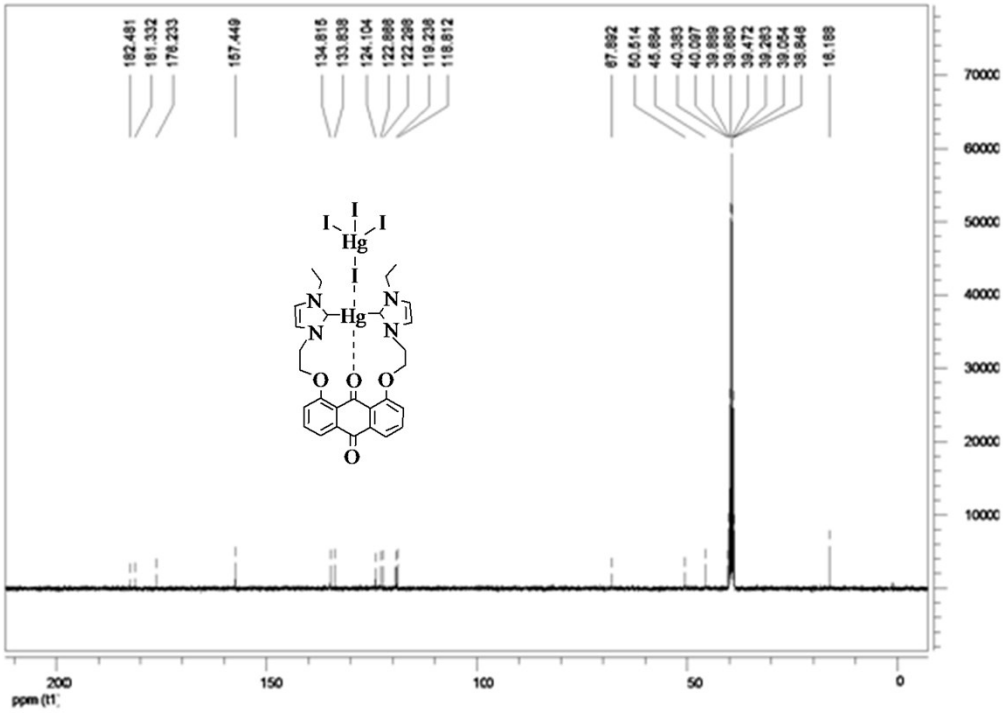

Fig. S19. The ^{13}C NMR (100 MHz, DMSO-d_6) spectrum for **3**.

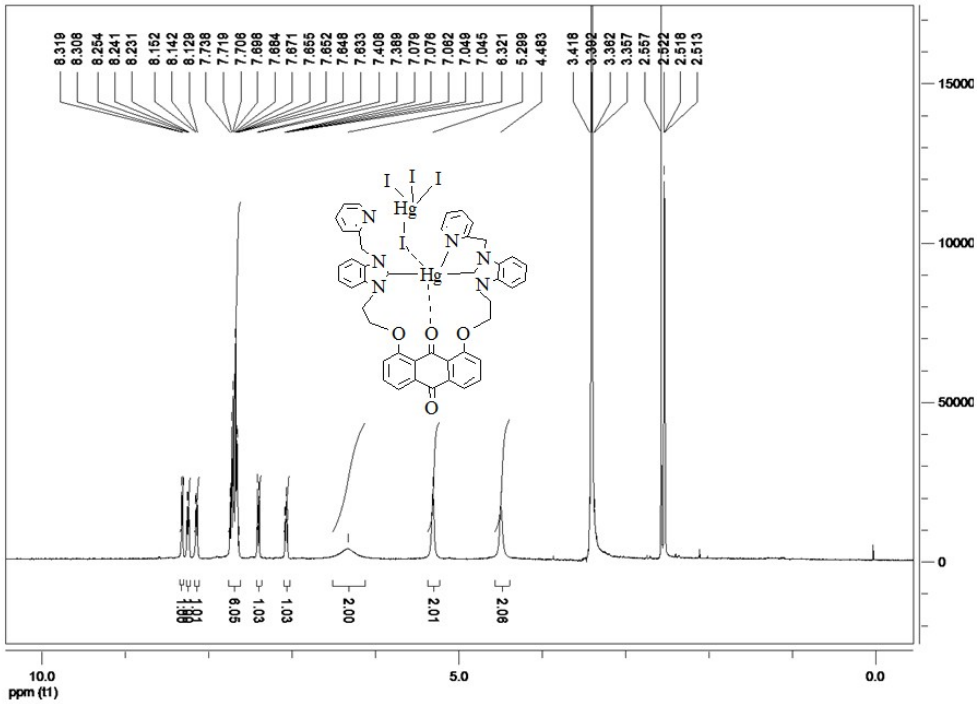

Fig. S20. The ^{1}H NMR (400 MHz, DMSO-d_6) spectrum for **4**.

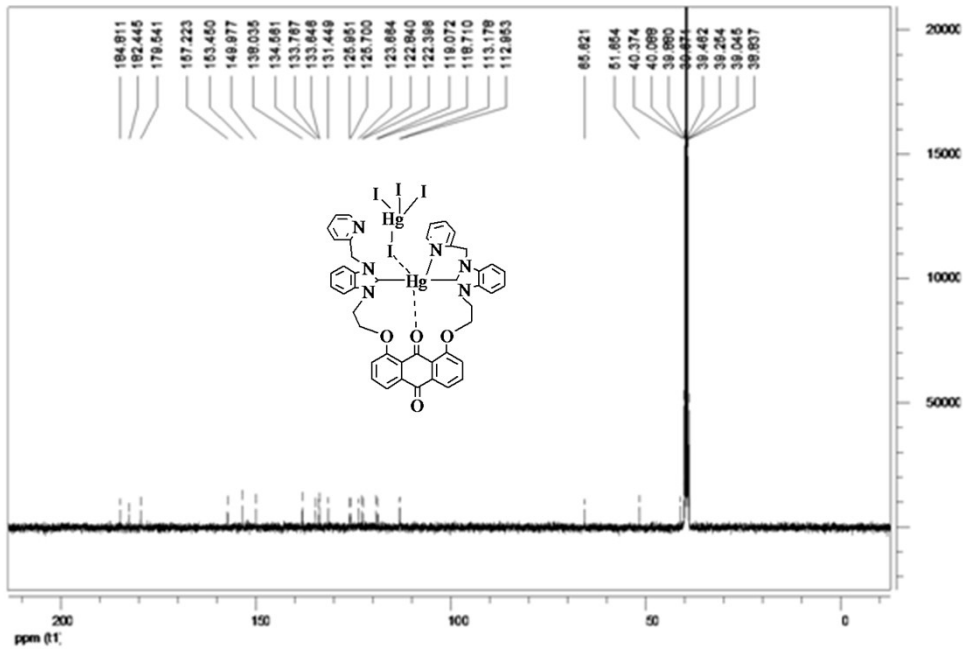

Fig. S21. The ^{13}C NMR (100 MHz, DMSO-d_6) spectrum for **4**.

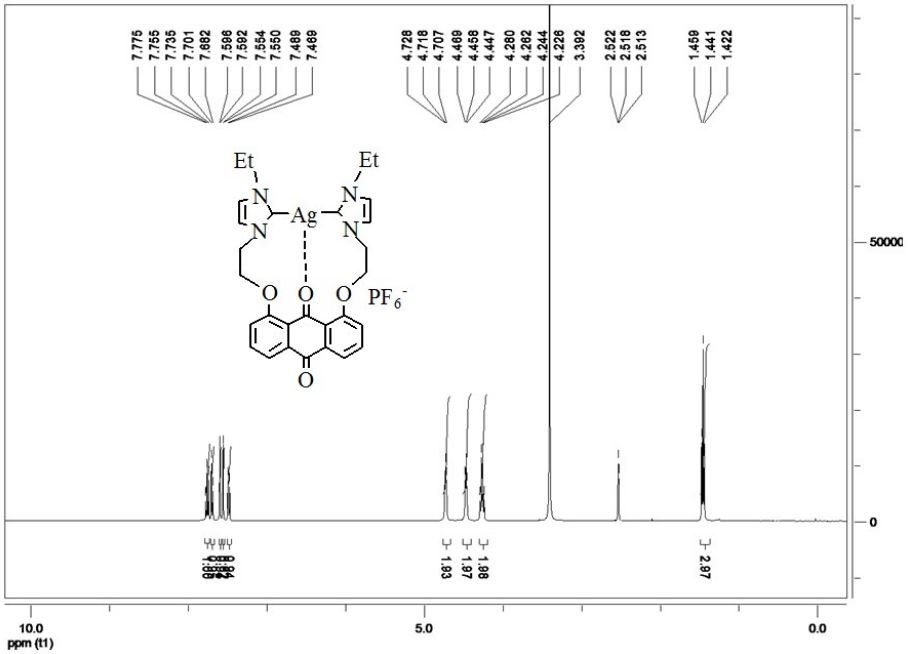

Fig. S22. The ^{1}H NMR (400 MHz, DMSO-d_6) spectrum for **5**.

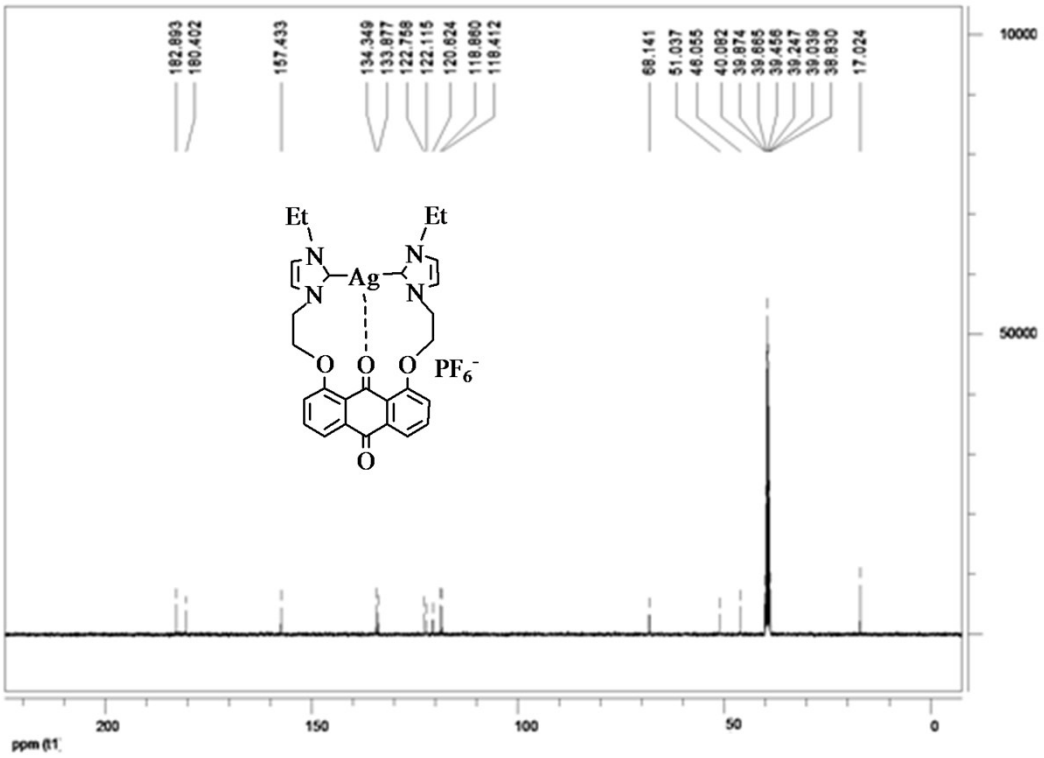

Fig. S23. The ^{13}C NMR (100 MHz, DMSO-d_6) spectrum for **5**.

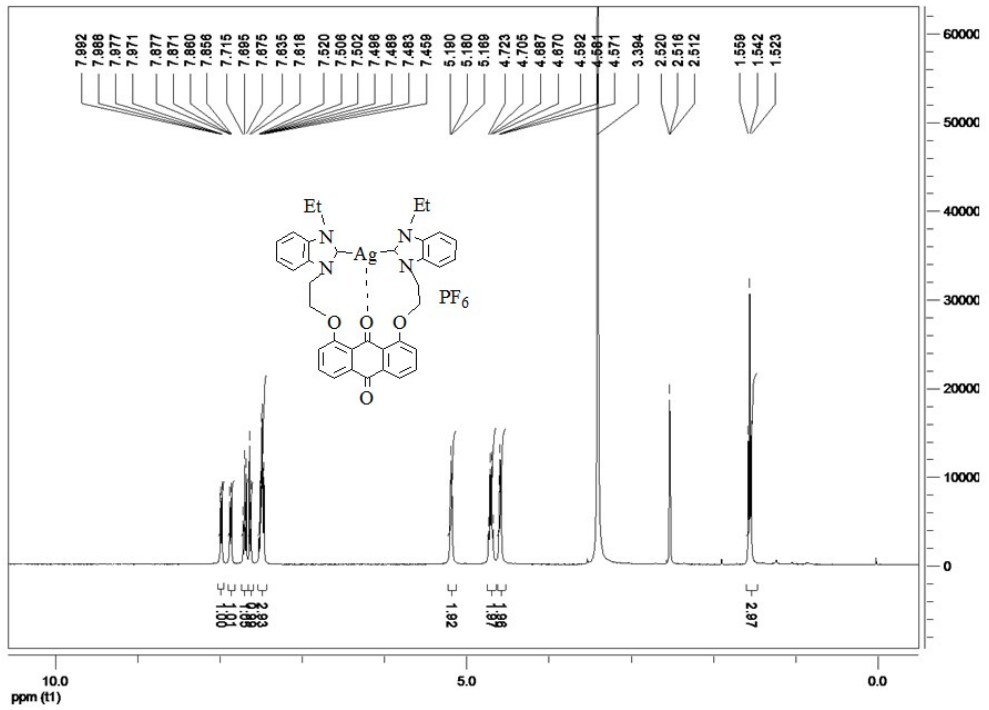

Fig. S24. The ^{1}H NMR (400 MHz, DMSO-d_6) spectrum for **6**.

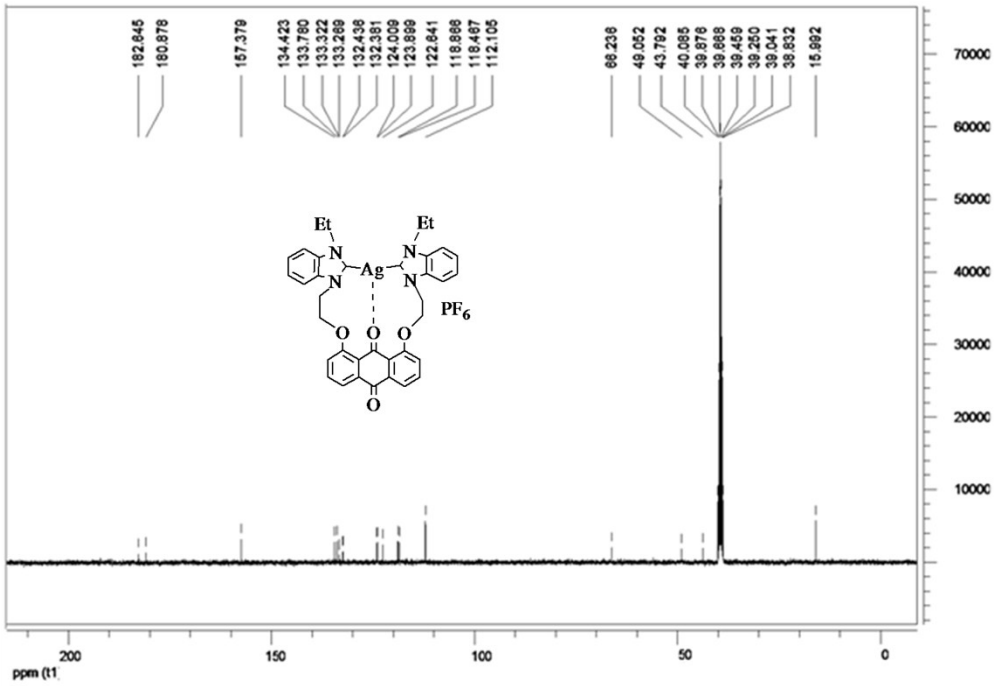

Fig. S25. The ^{13}C NMR (100 MHz, DMSO-d_6) spectrum for **6**.

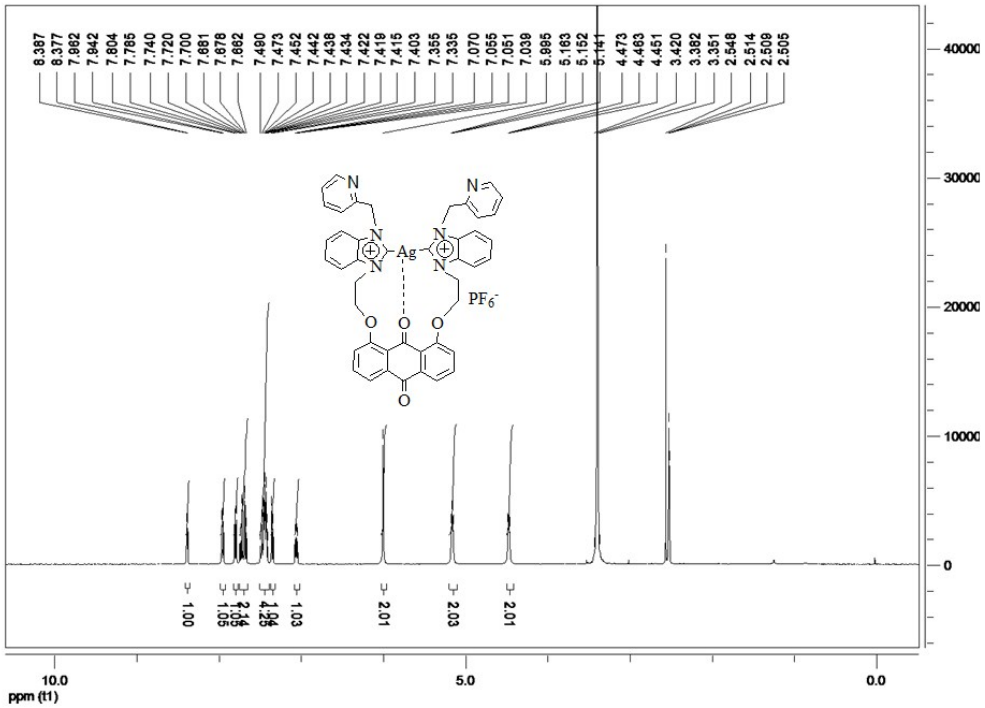

Fig. S26. The ^{1}H NMR (400 MHz, DMSO-d_6) spectrum for **7**.

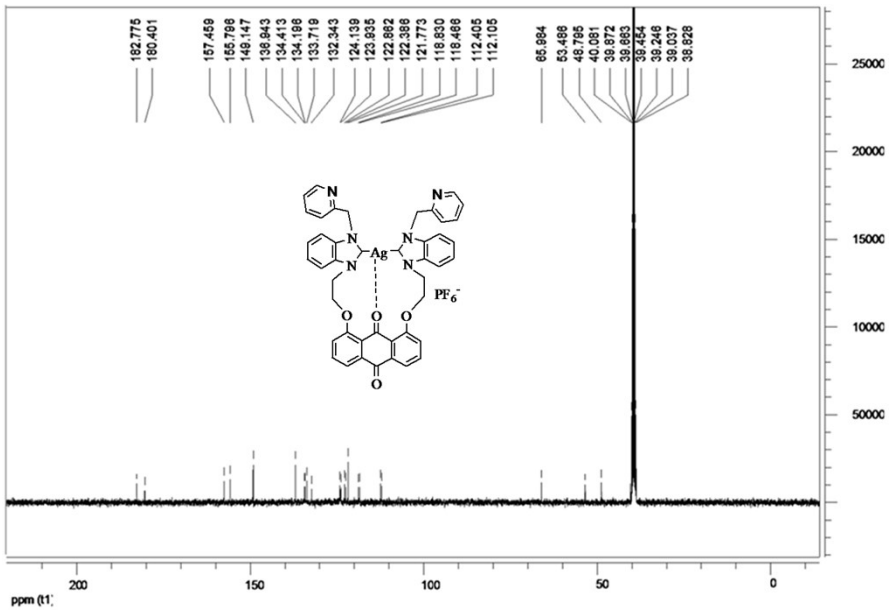

Fig. S27. The ^{13}C NMR (100 MHz, DMSO-d_6) spectrum for **7**.